

Fig. S1. Titration of MICA and ULBP2 concentrations for coating slides. pNK cells were incubated for 24 hours in wells coated with PLL (nonactivated) or with the indicated concentrations of MICA (left) or ULBP2 (right). IFN- γ (top) and CCL1 (bottom) release was then assessed by ELISA. The red asterisk indicates the ligand concentrations used in this study. Bars represent means \pm SD from two donors.

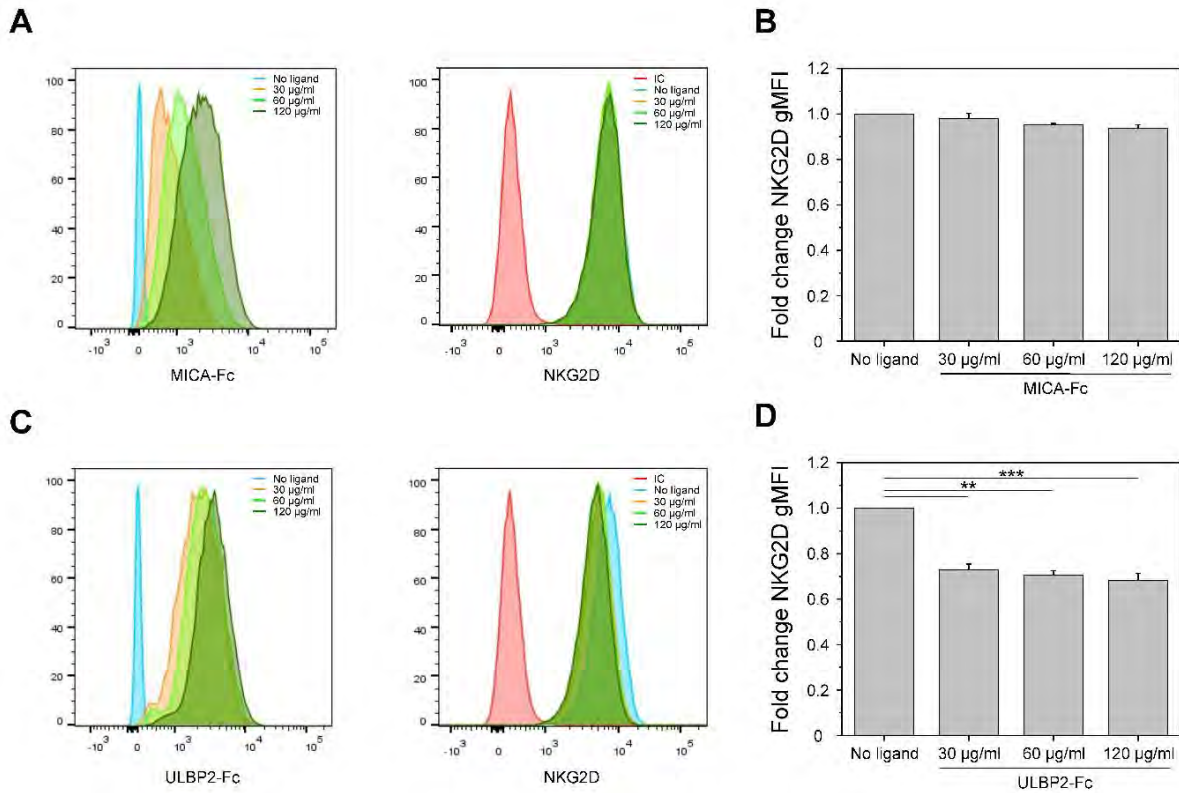


Fig. S2. The binding of NKG2D to MICA or ULBP2 does not block the binding of the NKG2D mAb 1D11 to the receptor. (A to D) NKL cells were left uncoated or coated with different concentrations of the indicated ligands at 37°C for 30 min, fixed with 4% PFA, stained with NKG2D antibody (clone 1D11) for 30 min at 4°C, and then analyzed by flow cytometry. (A and B) The effect of preincubation with MICA-Fc-Atto488 on the binding of mAb 1D11. (C and D) The effect of preincubation with ULBP2-Fc-Atto488 on the binding of mAb 1D11. (A and C, left) Histograms show the intensity of the MICA or ULBP2 fluorescent signal in cells coated with increasing amounts of ligands. (A and C, right) The intensity of the NKG2D fluorescent signal in the absence of MICA (A, blue histogram) or ULBP2 coating (C, blue histogram) was compared to the intensity of its fluorescent signal in the presence of 30 µg/ml (orange), 60 µg/ml (light green), or 120 µg/ml (dark green) MICA-Fc-Atto488 (A) or ULBP2-Fc-Atto488 (C) and to an isotype-matched control staining (A and C, red histogram). The bar graphs in (B) and (D) show the fold-change ± SD in the geometric mean fluorescence intensity (gMFI) of NKG2D from three independent experiments with cells precoated with MICA or ULBP2. ** $P < 0.01$ and *** $P < 0.001$ by one-way ANOVA with Tukey's post-test. Only statistically significant differences are indicated.

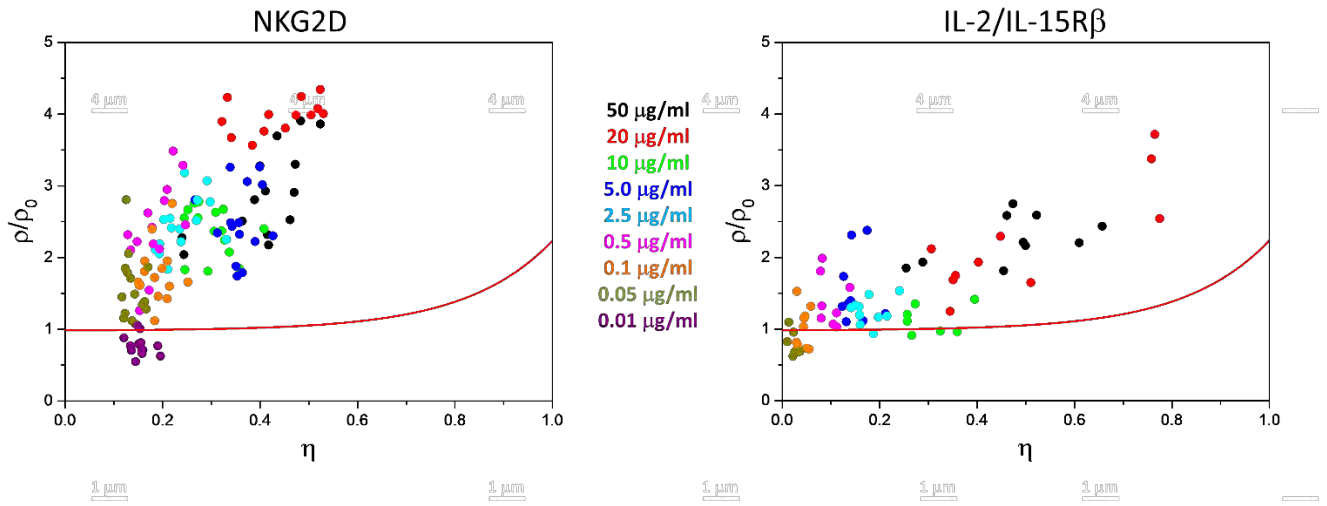


Fig. S3. Label density variation analysis of NKG2D and IL-2/IL-15R β . Normalized (mean density of localizations within the clusters density/relative area covered by the cluster masks) ρ/η curves from label-density variation analysis for NKG2D (left) and IL-2/IL-15R β (right). Cells were stained with NKG2D-Atto488 antibody or IL-2/IL-15R β -AF647 antibody at different labeling concentrations and imaged by dSTORM. Each data point represents a single cell and is color-coded by the antibody concentration used for labeling. Red lines indicate reference curves for a random distribution of molecules.

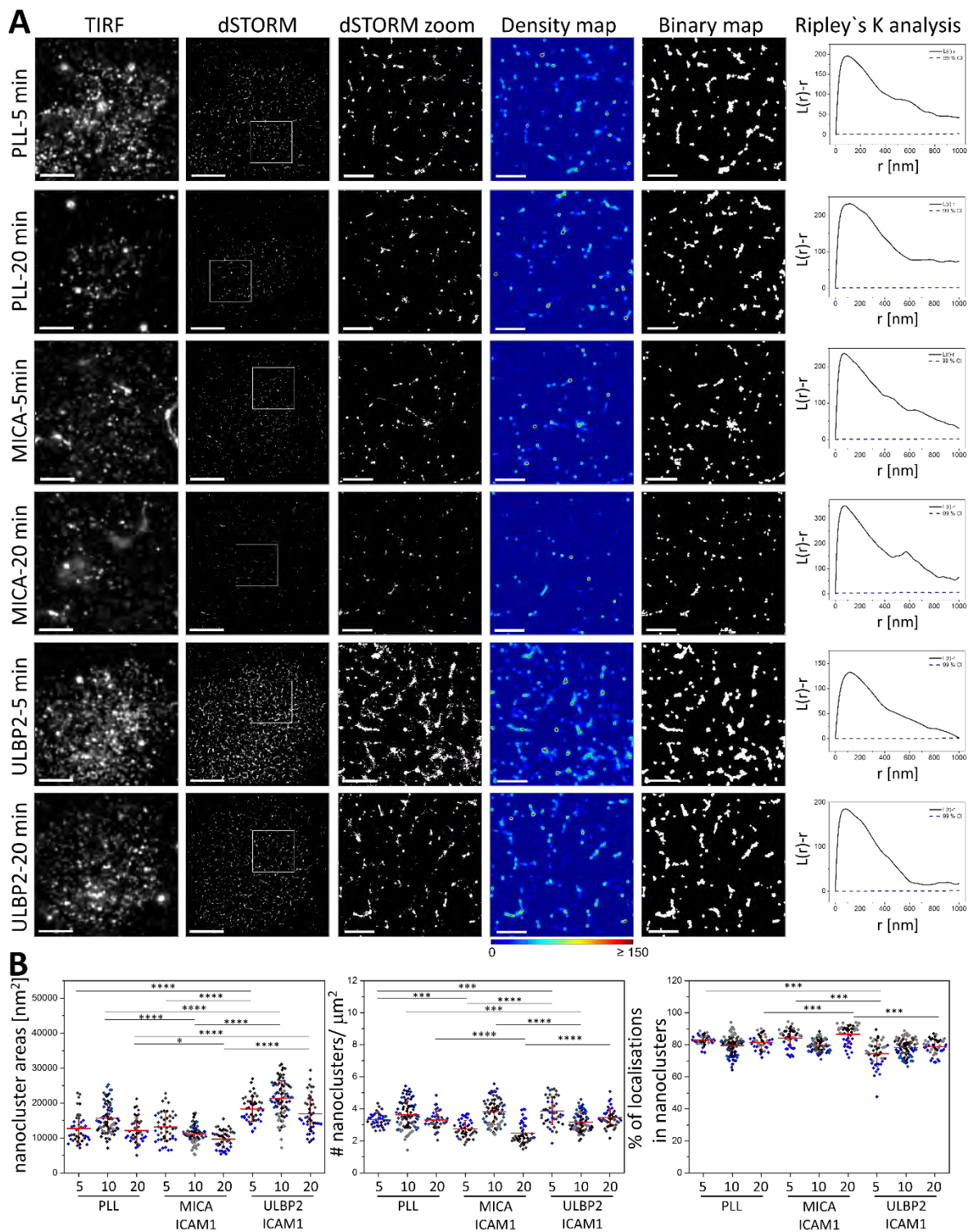


Fig. S4. Ligand-dependent reorganization of NKG2D at different times. (A) Representative TIRF and dSTORM images of NKG2D at the surface of pNK cells incubated for 5 or 20 min on slides coated with PLL (nonactivated), MICA and ICAM-1, or ULBP2 and ICAM-1, and stained with a fluorescently labeled specific mAb. Scale bars, 4 μm . Regions outlined by the white squares are magnified and shown with corresponding density images according to the pseudocolor scale bar, thresholded binary maps, and Ripley's K analysis. Scale bars, 1 μm . (B) Nanocluster areas (left), nanocluster density (middle), and percentage of localizations in nanoclusters (right) for NKG2D from data shown in (A) were calculated by subjecting dSTORM data to spatial point-pattern analysis and thresholding. Each symbol represents the median of several 5 $\mu\text{m} \times 5 \mu\text{m}$ regions from the same cell. Horizontal lines and errors represent means \pm SD. Data for the 10-min time point is from Fig. 1. Data are from a minimum of 40 cells from a minimum of three independent donors. Each color represents one donor. * $P < 0.05$, *** $P < 0.001$, and **** $P < 0.0001$ by one-way ANOVA with Tukey's post-hoc test in (B, left and middle), and Kruskal-Wallis with Dunn's post-hoc test in (B, right). Nonsignificant differences are not indicated.

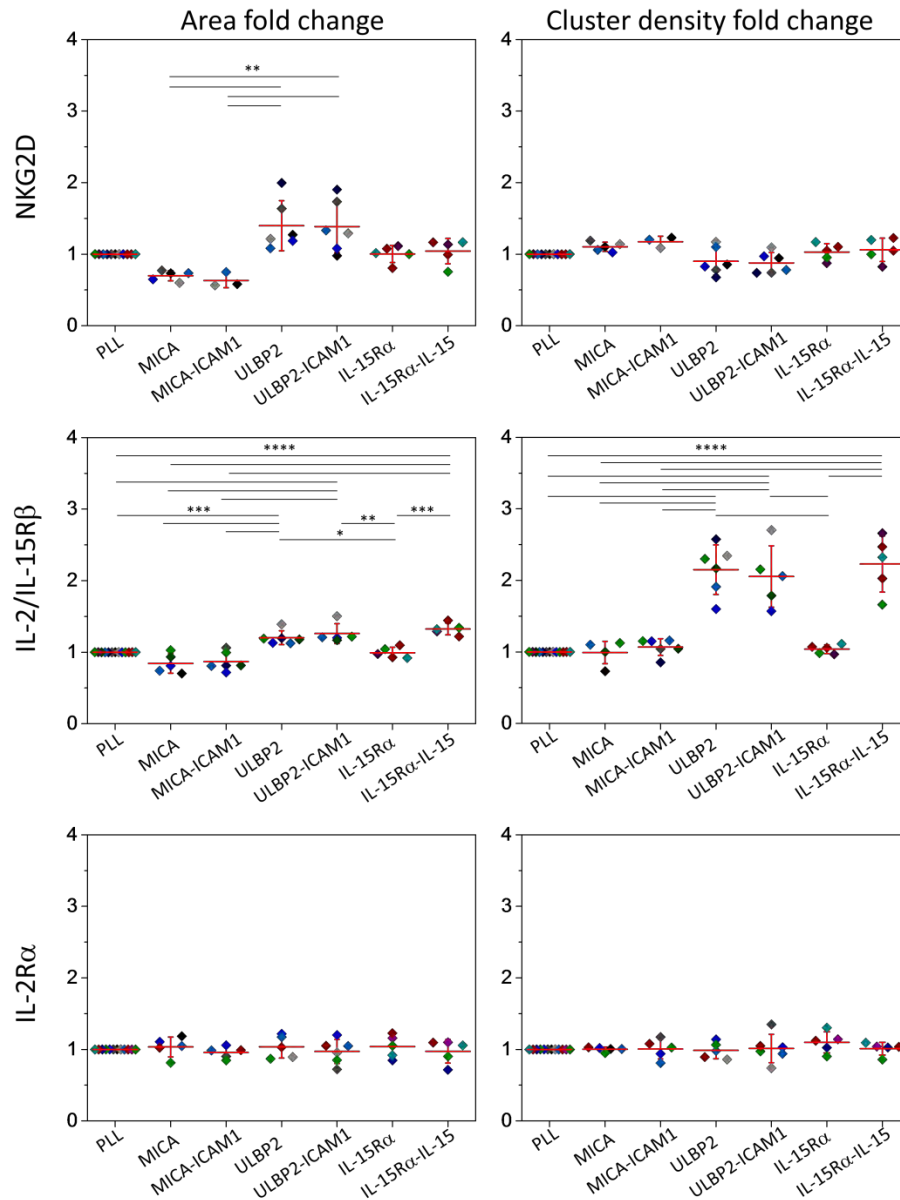


Fig. S5. Fold change in the nanoscale organization of NKG2D, IL-2/IL-15R β , and IL-2R α nanoclusters. Fold-changes in nanocluster area and density for NKG2D (top), IL-2/IL-15R β (middle), and IL-2R α (bottom) on pNK cells after a 10-min incubation with the indicated ligands. For each parameter, the fold-change was calculated by normalizing the average of the medians per condition to the average of the medians in the nonactivated condition (data are from Figs. 1, 3, and 4, and fig. S8). Each color represents the fold-change for one donor. Horizontal lines and errors represent means \pm SD. Data are from a minimum of three independent donors. * P < 0.05, ** P < 0.01, *** P < 0.001, and **** P < 0.0001 by one-way ANOVA with Tukey's post-hoc test. Nonsignificant statistical differences are not indicated.

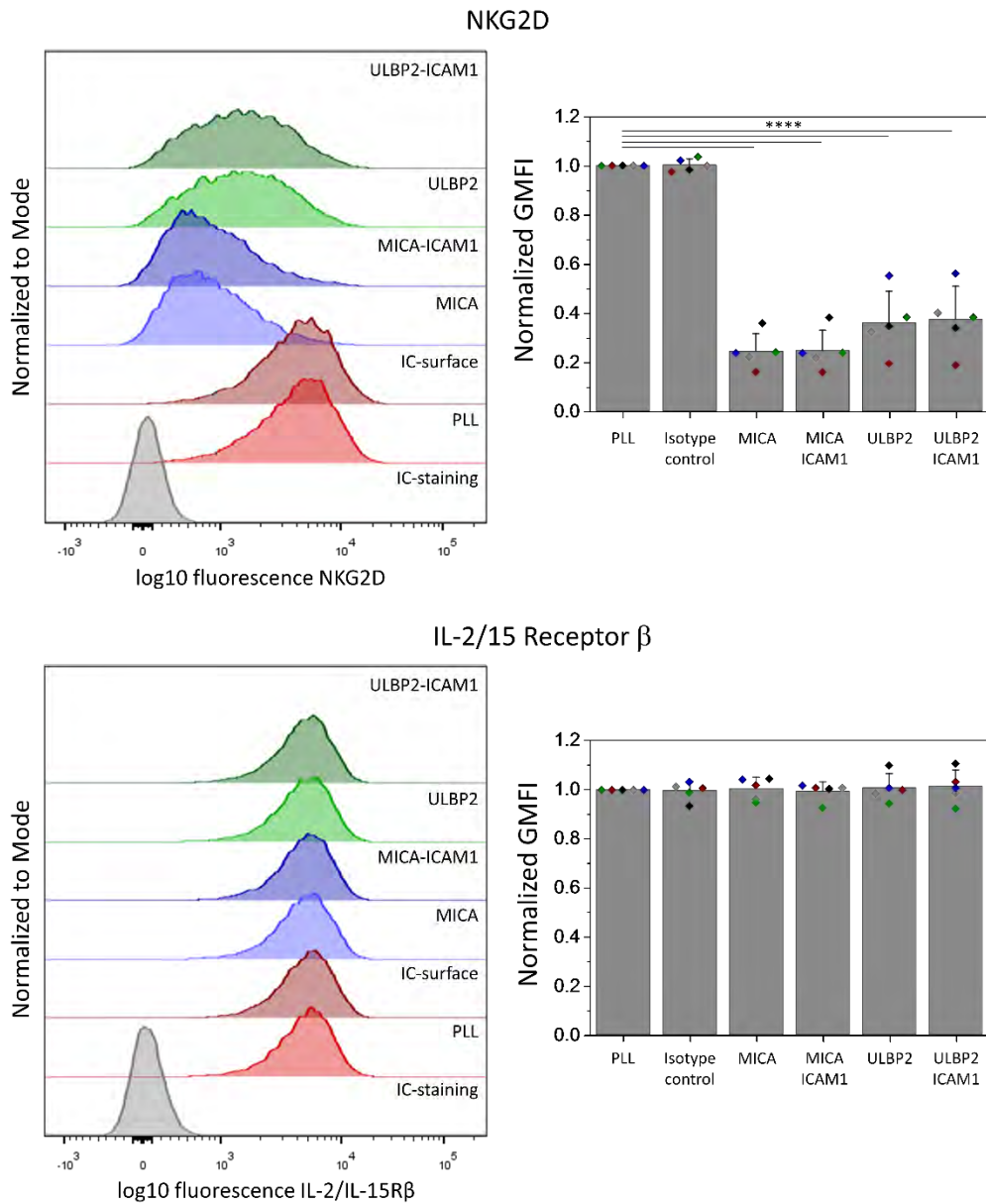


Fig. S6. Surface expression analysis of NKG2D and IL-2/IL-15R β . pNK cells were incubated for 10 min in wells coated with PLL (nonactivated), isotype control, MICA, MICA and ICAM-1, ULBP2, or ULBP2 and ICAM-1, stained, and analyzed by flow cytometry. The expression of NKG2D or IL-2/IL-15 β in live CD56⁺ cells was assessed with APC-labeled specific antibodies. For each receptor, representative histograms of specific staining are compared with an isotype-matched control (gray). The geometric mean fluorescence intensity (GMFI) for NKG2D and IL-2/IL-15R β under the indicated conditions is shown next to the histograms. Bars represent means \pm SD of five independent donors. Each color represents the mean of one donor. **** $P < 0.0001$ by one-way ANOVA with Tukey's post-hoc test. Nonsignificant differences are not indicated.

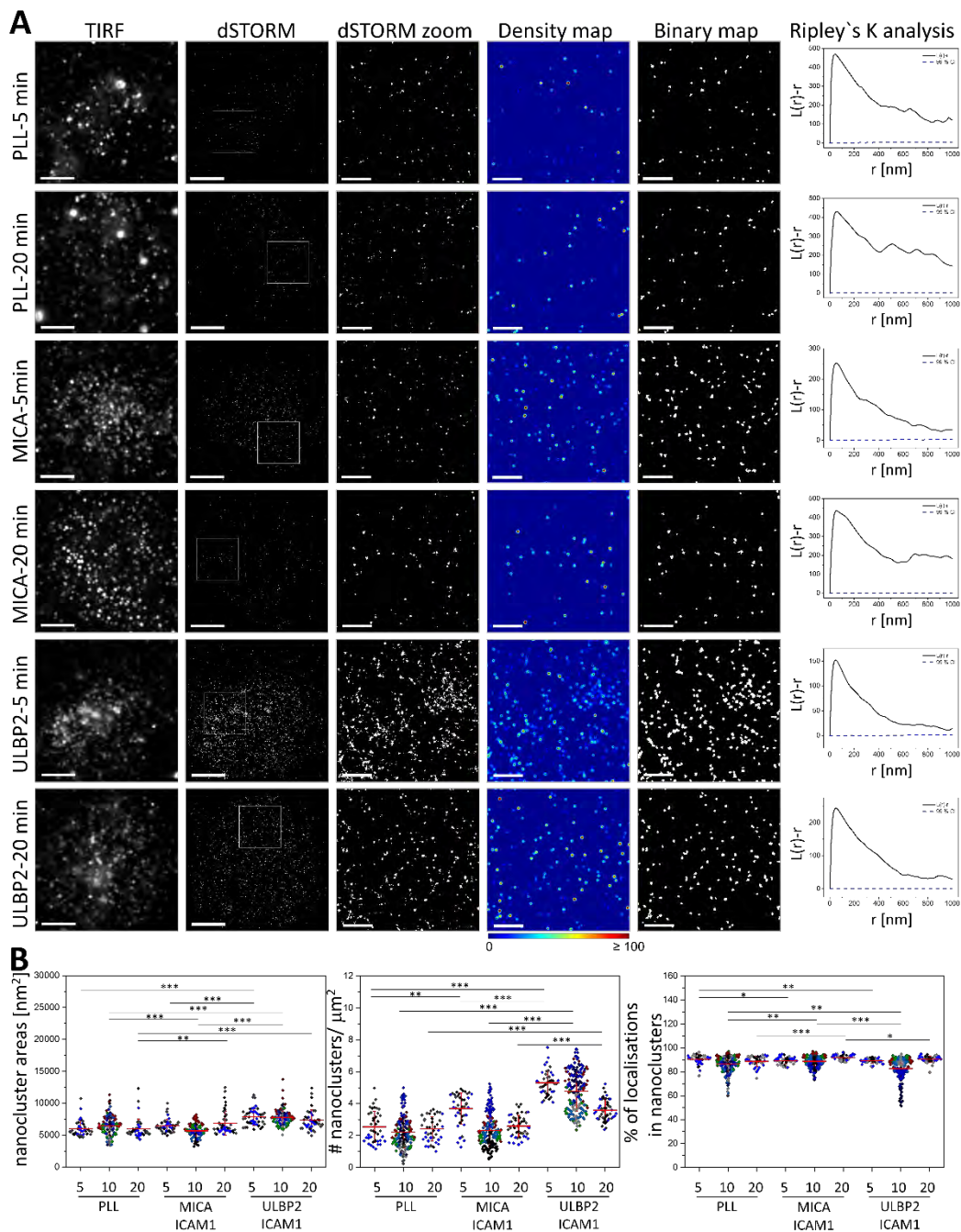


Fig. S7. Ligand-dependent reorganization of IL-2/IL-15R β at different times. (A) Representative TIRF and dSTORM images of IL-2/IL-15R β at the surface of pNK cells incubated for 5 or 20 min on slides coated with PLL (nonactivated), MICA and ICAM-1, or ULBP2 and ICAM-1, and stained with a fluorescently labeled specific mAb. Scale bars, 4 μm . Regions outlined by the white squares are magnified and shown with corresponding density images according to the pseudocolor scale bar, thresholded binary maps, and Ripley's K analysis. Scale bars, 1 μm . (B) Nanocluster areas (left), nanocluster density (middle), and percentage of localisations in nanoclusters (right) for IL-2/IL-15R β from data shown in (A) were calculated by subjecting dSTORM data to spatial point-pattern analysis and thresholding. Each symbol represents the median of several 5 $\mu\text{m} \times 5 \mu\text{m}$ regions from the same cell. Horizontal lines and errors represent means \pm SD. Data for the 10-min time point are from Fig. 3. Data are from a minimum of 40 cells from a minimum of three independent donors. Each color represents one donor. * $P < 0.05$, *** $P < 0.001$, and **** $P < 0.0001$ by Kruskal-Wallis with Dunn's post-hoc test. Nonsignificant differences are not indicated.

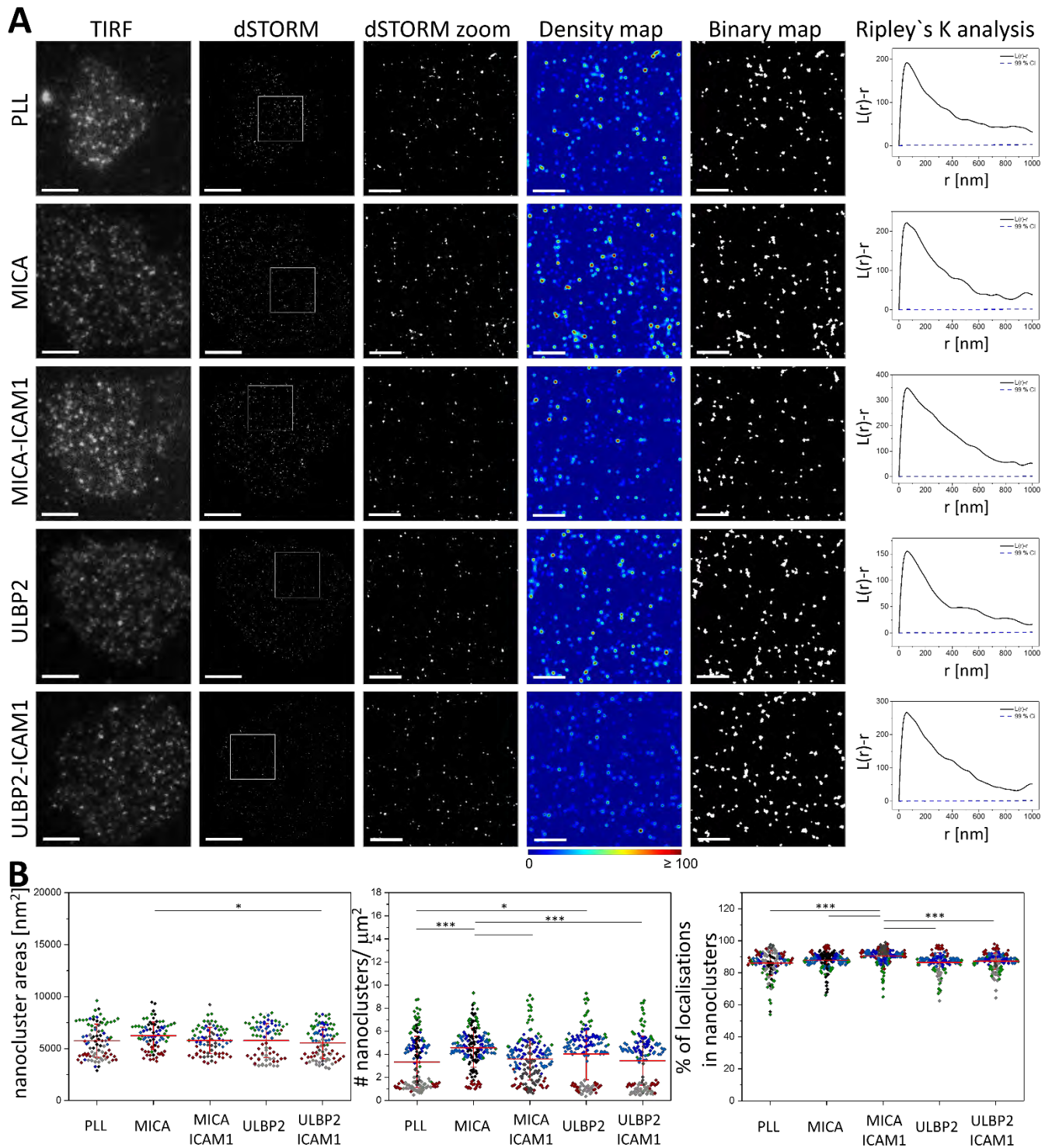


Fig. S8. The nanoscale organization of IL-2R α remains unaltered upon ligation of NKG2D. (A) Representative TIRF and dSTORM images of IL-2R α at the surface of pNK cells incubated for 10 min on slides coated with PLL (nonactivated), MICA, MICA and ICAM-1, ULBP2, or ULBP2 and ICAM-1, and stained with a fluorescently labelled specific mAb. Scale bars, 4 μm . Regions outlined by the white squares are magnified and shown with corresponding density images according to the pseudocolor scale bar, thresholded binary maps, and Ripley's K analysis. Scale bars, 1 μm . (B) Nanocluster areas (left), nanocluster density (middle), and percentage of localizations in nanoclusters (right) for IL-2R α from data shown in (A) were calculated by subjecting dSTORM data to spatial point-pattern analysis and thresholding. Each symbol represents the median of several 5 $\mu\text{m} \times 5 \mu\text{m}$ regions from the same cell. Horizontal lines and errors represent means \pm SD. Data are from a minimum of 80 cells from a minimum of three independent donors. Each color represents one donor. * $P < 0.05$ and *** $P < 0.001$ by one-way ANOVA with Tukey's post-hoc test in (B, left) and Kruskal-Wallis with Dunn's post-hoc test in (B, middle and right). Nonsignificant statistical differences are not depicted in the graphs.

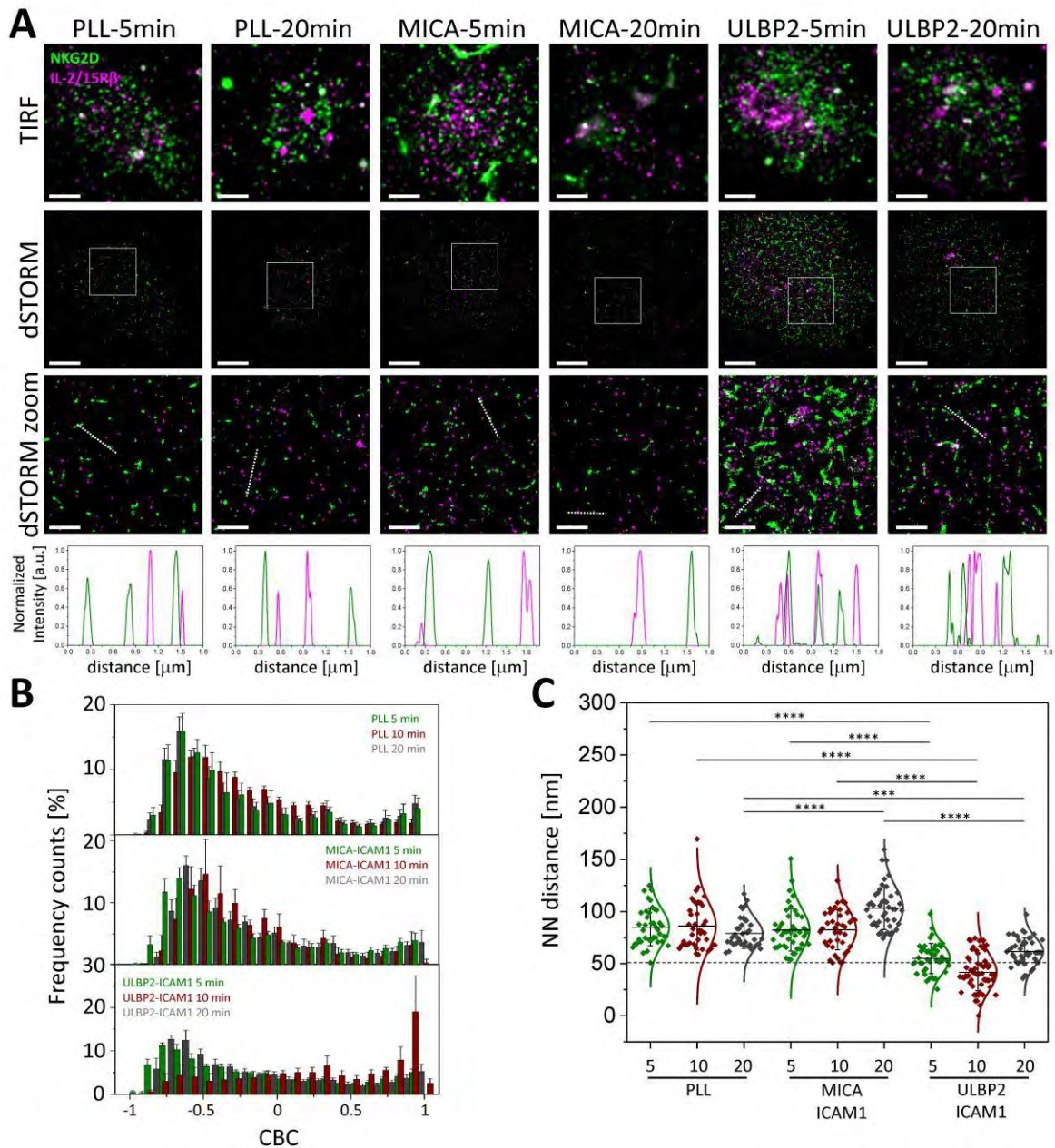


Fig. S9. Time-dependent association between NKG2D and IL-2/IL-15R β nanoclusters induced by ULBP2. (A) Representative TIRF and dSTORM images showing NKG2D and IL-2/IL-15R β on pNK cells incubated for 5 or 20 min on slides coated with PLL, MICA and ICAM-1, or ULBP2 and ICAM-1, and stained with fluorescently labeled specific mAbs conjugated with Atto488 (for NKG2D) or AF647 (for IL-2/IL-15R β). Scale bars, 4 μm . Regions outlined in white are magnified with relative fluorescence intensity profiles along the white lines. Scale bars, 1 μm . Colocalization between the channels is shown in white. (B) CBC histograms of the single-molecule distributions of the colocalization parameter for NKG2D and IL-2/IL-15R β in cells incubated as described in (A). Data are from a minimum of 10 cells from three independent donors. Bars represent means \pm SD. (C) Nearest-neighbor distance (NND) analysis from data shown in (A). Data are from a minimum of 40 cells from three independent donors. Each symbol represents the median NND of all paired single-molecule localizations from one cell. Lines and errors represent means \pm SD. *** $P < 0.001$ and **** $P < 0.0001$ by one-way ANOVA with Tukey's post-hoc test. Nonsignificant statistical differences are not depicted in the graphs.

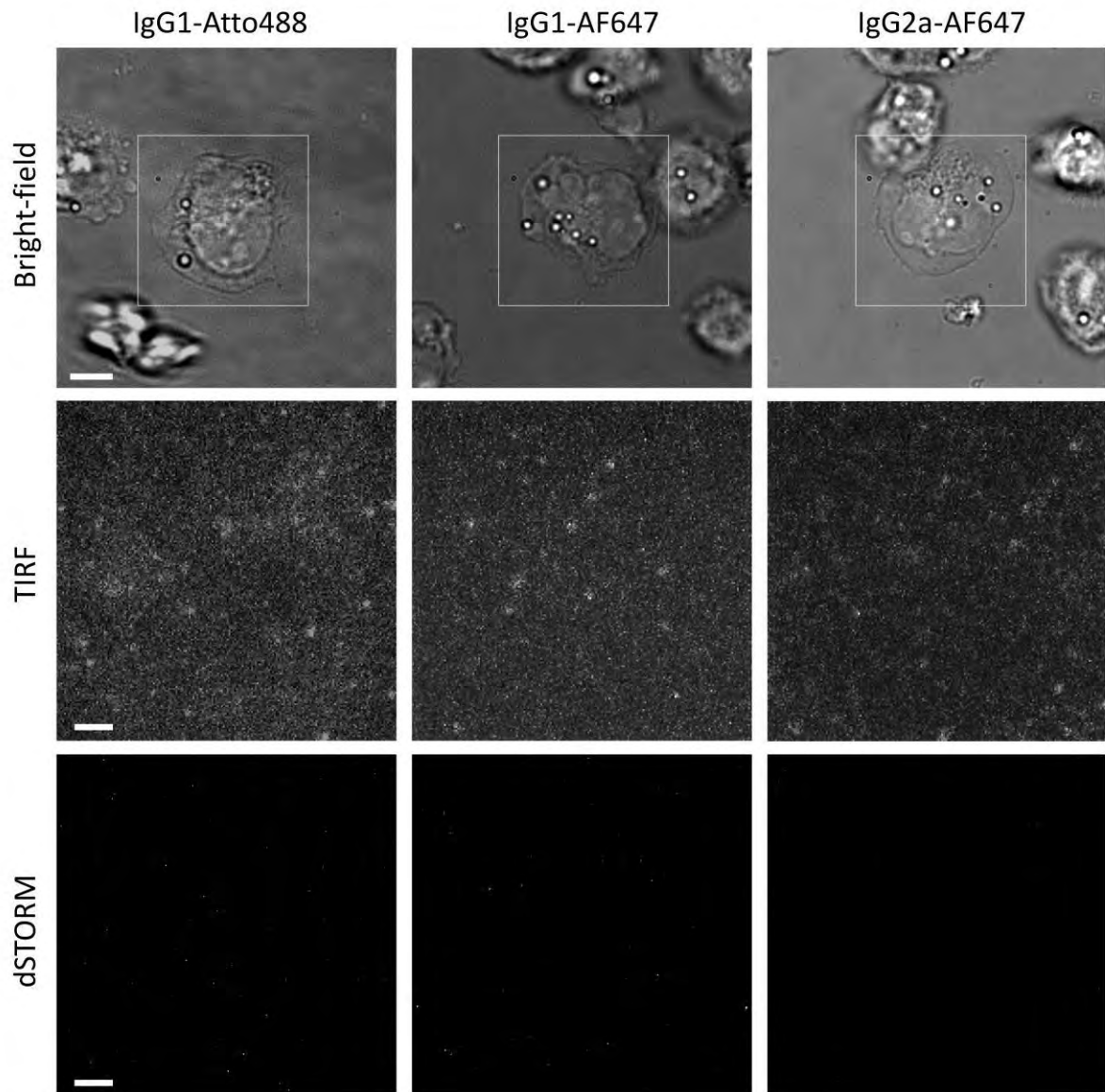


Fig. S10. Isotype-matched control staining. Representative bright-field (scale bar, 5 μm), and TIRF and dSTORM (scale bars, 2 μm) images corresponding to the regions outlined by the white squares showing pNK cells stained with isotype-matched control antibodies for all antibodies used in this study.